

Studying the Z Boson with the ATLAS Detector at the LHC ¹

Q. Coc and P. Huth

Abstract: In this experiment we measure the mass and width of the Z -Boson using pre-selected data measured by the ATLAS detector at the LHC in 2012 along with Monte Carlo (MC) simulations of Standard Model processes [cite]. The comparison of both data sets, measurements and MC, reveal data points generated by secondary processes irrelevant for our purposes, which were consequently filtered out. By fitting the convolution of a Gaussian and a Breit-Wigner distribution to the filtered data we determine $m_Z = 90.629(5)$ GeV and $\Gamma = 3.258(21)$ GeV. Both values display a significant deviation from the values reported by the Particle Data Group ² of $\sigma_{M_Z} = 27.11$ and $\sigma_{M_Z} = 36.09$.

Als besondere Auswertung testiert: Datum, Unterschrift:

¹Experiment FP94 performed the 4th Nov. 2024. Supervisor: Ruiz, Miguel

²S. Navas et al. (Particle Data Group), Dec. 2024.[\[Online\]](#)

1 Introduction

The electroweak theory, unification of the electromagnetic and weak forces, was developed during the 70's by S. Glashow, A. Salam and S. Weinberg. It's lagrangian is symmetric under $SU(2)_L \times U_Y$ local gauge transformations and thus gives rise to 4 gauge bosons. After spontaneous symmetry breaking (SSB) the Goldstone-bosons corresponding to the weak interaction, W^+ , W^- and Z , acquire large masses while the boson mediating the electromagnetic, photon γ , remain massless. Five years after the publication of the electroweak theory, the W^\pm and Z boson were discovered experimentally.

The W and Z bosons were found at CERN. First, in the study of proton-antiproton collisions at the SPS and secondly in the analysis of electron-positron collision at the LEP. The latest precision measurements carried out by the ATLAS detector at the LHC.

The properties of the Z boson are mainly studied using the Drell-Yan process. It refers to the three-level Feynman diagram of a pair of quarks annihilating and forming a short lived virtual γ or Z bosons which subsequently decays into a pair of leptons: $q_c \bar{q}_c \rightarrow l \bar{l}$. From the properties of the final leptons it is possible to deduce information about the mediating boson. Since, such processes occur during highly energetic $p\bar{p}$ scattering, further processes and types of particles may contribute to the detected number of leptons.

Particle detection can be broken-down into three parts: reconstruction, calibration and identification. For this purpose the detector implements different components, namely: inner detector (ID), calorimeter cluster (ECAL and HCAL), a muon spectrometer (MS) and a magnet system.

For the identification of electrons, the reconstruction algorithm uses information from the innermost layer (ID) and the calorimeter cluster. Due to the small ionization generated by muons, their reconstruction relies on the tracks from the ID and MS systems. These tracks are then fitted either by a e^- or a μ hypothesis to select candidates. The calibration is done by setting an appropriate energy scale with help of simulations, e.g MC simulation. The candidates selected during this first stage are impure and can be corrected by the likelihood (LC) method, which quantize the probability of an event to be an electron or muon, thus serving as an identification algorithm. Finally, the relevant particles can be selected by applying isolation requirements to further filter out leptons coming from undesired processes.

2 Procedure and Results

In the experiment FP91 we analyse properties of the Z boson using measurements taken in 2012 by the ATLAS experiment, which were published for educational use^{3 4}. The integrated luminosity is $\mathcal{L}_{int} = 1.0070(19) \text{ fb}^{-1}$ and the a center of mass energy $\sqrt{s} = 8 \text{ TeV}$. Additionally, we use MC simulations which were provided by our supervisor. Both of the datasets, measurements and MC, are tightly preselected by different isolation requisites.

We start the experiment by analysing different properties of the measured data. Among them, the position of the primary vertex along the z-Axis, the number of leptons produced, the azimuthal angle, pseudorapidity and p_T distributions.

By plotting the number of leptons of each event in the measured data set we can see that most of the preselected events contain one lepton as final state. Such events are dominated by W process, e.g. $q \bar{q} \rightarrow W^+ \rightarrow e^- \bar{\nu}_e$, revealing that most of the events are not relevant for studying the Z boson. These kind of events can be filtered out by imposing the number of leptons to be $n_l \geq 2$.

For a further analysis of the measured data we calculate the invariant mass of the two leading leptons and compare it to the invariant mass of the $Z \rightarrow e^- e^+$ simulations, see 1. From theory, we would expect a resonance curve centred around the expected mass of the Z boson, $\sim 91.187 \text{ GeV}$. Our predictions are met by the invariant mass distribution of the MC simulations. While the mass distribution of the preselected data shows a predominant resonances peak around M_Z , three extra

³”Review Studies for the ATLAS Open Data 8 TeV datasets, tools and activities”, CERN, Dec. 2024.[Online]

⁴”Review Studies for the ATLAS Open Data Set”, CERN, Dec. 2024.[Online].

resonance curves are visible at $M < 50$ GeV. These peaks correspond to bottom and charm resonances which likely decay into leptons. These events are irrelevant for our purposes.

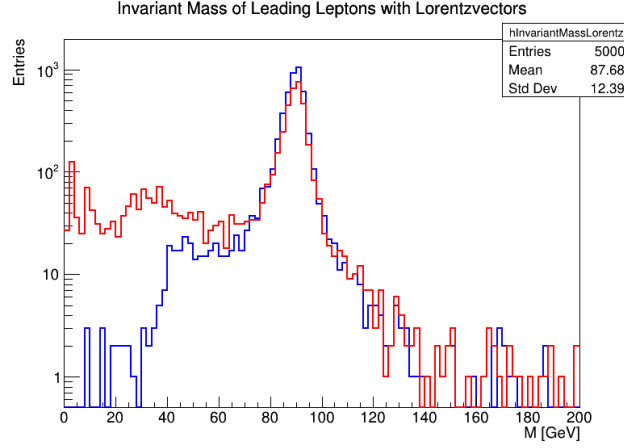


Figure 1: Leading lepton’s invariant mass of measured data (red) compared to the invariant mass of Monte Carlo simulation of $Z \rightarrow e^- e^+$ (blue). The invariant mass was computed using calculated ROOT’s `TLorentzVector` class.

After these two observations it is clear that the preselected data has to be filtered out to leave only the relevant Drell-Yan processes. For this purpose we impose isolation requirements to the measured data sets. To keep track of how many events are discarded by each applied criteria we plot a so called cut flow. Additionally, we plot the invariant mass distribution of the filtered data. We do this for Z process with e , μ or τ pairs as final state. These plots are presented in Fig 3.

The bins on the cut-flow histogram represent applied isolation requirements. These constraints are applied consecutively from left to right. The y-axis shows the remaining number of events after the requirement on the x-axis was applied. Due to already harshly filtered data which is being used, no major change is generated by the first three conditions. For the same reason, there is no decrease in the number of events in the case of τ when Tight ID is applied. The number of events is unchanged between Lepton PDGID and Opposite Charges. For the case of τ , Trigger Fired was omitted, since the data lacks a `trigT` attribute. For the Isolation requirement we apply an isolation of 0.1.

From the cut flow histograms it is clear that the Lepton PDGID and Isolation requirements generate the biggest decrease in number of events. We conclude that cut on lepton-level constraints are more efficient than cut at event-level. Lepton-level cuts are specialized for the process to be analysed and thus are more efficient to filter out undesired events.

The corrected mass distributions from e and μ now show a prominent resonance peak around the expected mass of the Z boson. In contrast, the events filtered as τ show an asymmetric distribution which tends to ~ 80 GeV. The reason for this behaviour is due to the properties of τ . Since these particles are unstable, they don’t reach the detector and decay into other particles. Hence, the filtered events contain the leptons coming from τ decays and don’t give high quality information to study the Z boson. These kind of events are able to be identified by the p_T of the resulting neutrinos, $\nu_{e/\mu}$ and ν_{τ} , but are irrelevant for this experiment.

To study the properties of the Z boson we will only consider the e and μ pair events. For this reason we merge the filtered $Z \rightarrow e^- e^+$ and $Z \rightarrow \mu^- \mu^+$ events into a single histogram and compare it to the invariant mass distribution of the MC simulations, see left image in Fig. 3. The plot demonstrates the great agreement between the measured events and the MC simulations.

Next, we compare the fit of a Gauss distribution, a relativistic Breit-Wigner (BW) distribution and the resulting distribution from the convolution of the former ones. On one hand, due to the large number of data points in our data set and the nature of the measured events, the central limit theorem dictates that the distribution of the measurements tends to a normal distribution. On the other hand, from QFT we know that the mass distribution of an unstable particle in vacuum can accurately be

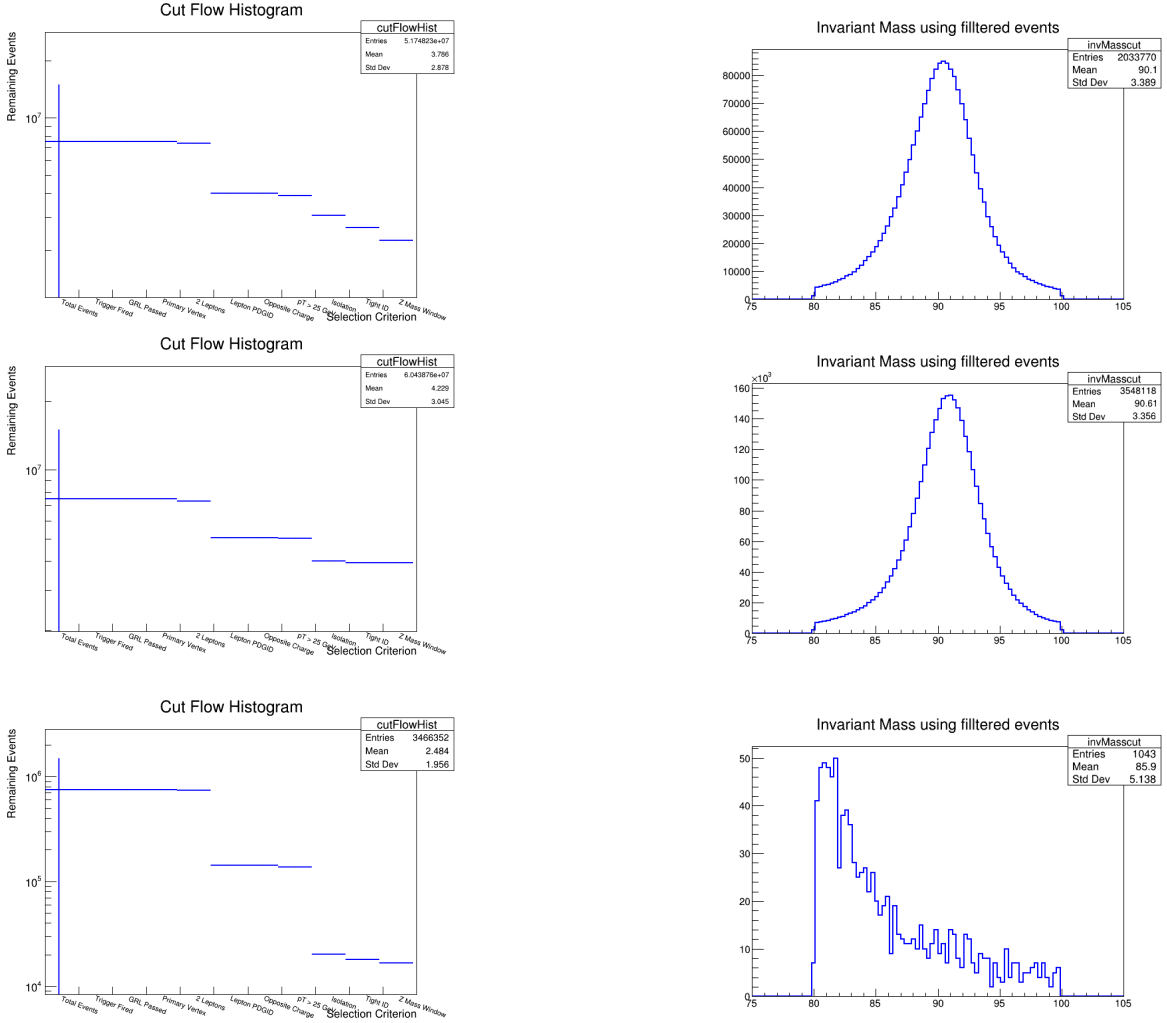


Figure 2: Cut flow from e , μ and τ events and invariant mass distribution of filtered data. Each row corresponds to the plots of each lepton: first row e , the second row μ and the third τ . The cut flow histogram is display on the first column and the invariant mass distribution on the left.

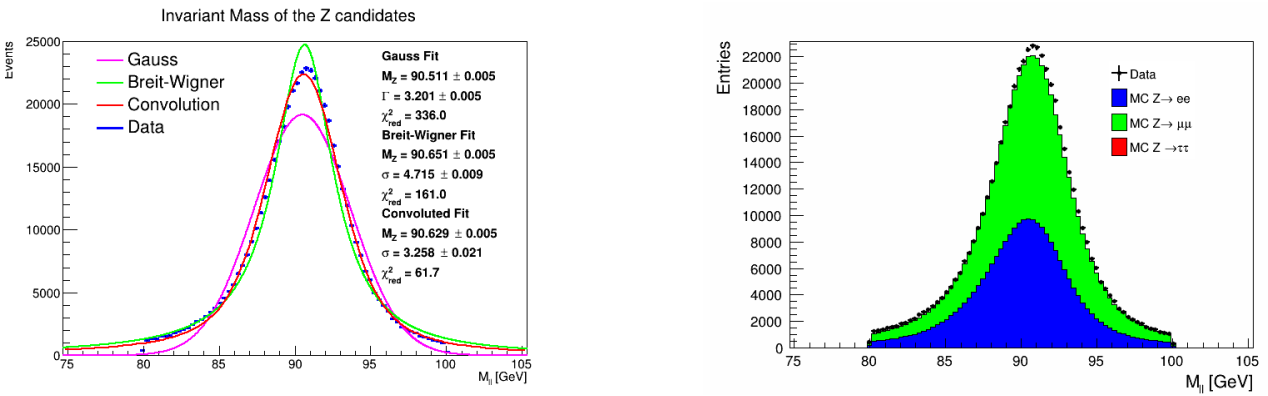


Figure 3: Right: Selected data (blue) and the fit of three distributions: (violet) Gauss-distribution, (green) Breit-Wigner Distribution and (red) convolution of a Gauss and Breit-Wigner distribution. Left: Merge of filtered electron and muon pair events (black cross) compared to MC simulations for $Z \rightarrow l\bar{l}$ processes.

described by a relativistic Breit-Wigner distribution. The left image in Fig. 3 makes clear that the BW renders a better fit compared to the gaussian fit. Nevertheless the χ^2/dof is rather high. The convolution of both distribution shows a clear advantage over the individual fits, since it take into consideration the statistical and physical nature of the measured data.

From the fitted convolution, we are able to determine the mass of the Z boson and its width. The experimentally found values are presented in Tab. 1 along with the values reported by the Particle Data Group ⁵. Even with the convolution yielding a better fit than any single distribution, we notice that the resulting mass and width for the Z boson deviate significantly when compared to the values reported by PDG. We will discuss possible error sources in the discussion.

Table 1: Comparison of measured quantities with values reported by the Particle Data Group (PDG).

	PDG	Fit parameter	Deviation
M_Z [GeV]	90.629(5)	91.1880(20)	27.11
Γ [GeV]	3.258(21)	2.4955(23)	36.09

As a final part of our analysis we use the tag-and-probe method to determine the efficiency of the different isolation requirements used for the selection of the data. Using the characteristic signature of $Z \rightarrow ee$ decays, the tag-and-probe method aims to produce a clean and unbiased sample to deduce said efficiency.

We introduce tight constraints upon one of the two electrons produced by the decay, in a simmlar fashion to the cut flow. The electron upon which these constraints are bestowed is the 'tag'. If it complies with the set restrictions, the second electrons, or the 'probe', will be further considered. Previous criteria on the invariant mass do still hold true and aim to further reduce background.

The efficiency is then obtained via the fraction of probe candidates that satisfy all criteria. The results of this analysis is depicted in Fig.4 against p_T .

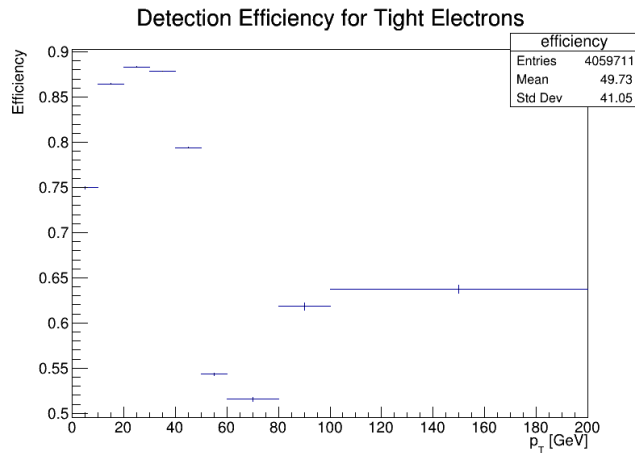


Figure 4: Detection Efficiency for tight Electrons obtained via the Tag-and-Probe method.

3 Summary

4 Critical discussion

⁵S. Navas et al. (Particle Data Group), Dec. 2024.[\[Online\]](#)